CLNS 98/1583
CLEO 98-14

Search for Exclusive Rare Baryonic Decays of B Mesons

CLEO Collaboration

(November 24, 1998)

Abstract

We report the results of a search for the rare baryonic decay modes $B^0 \to \Lambda\overline{\Lambda}$, $B^+ \to \overline{\Lambda}p$, $B^0 \to \overline{\Lambda}p\pi^-$, and $B^0 \to p\overline{p}$ (and their charge conjugate states) using 5.8×10^6 $B\overline{B}$ pairs collected with the CLEO detector. We see no statistically significant signals in any of these modes and set 90% confidence level upper limits on their branching fractions, $\mathcal{B}(B^0 \to \Lambda\overline{\Lambda}) < 3.9 \times 10^{-6}$, $\mathcal{B}(B^+ \to \overline{\Lambda}p) < 2.6 \times 10^{-6}$, $\mathcal{B}(B^0 \to \overline{\Lambda}p\pi^-) < 1.3 \times 10^{-5}$, and $\mathcal{B}(B^0 \to p\overline{p})$ $< 7.0 \times 10^{-6}$.

T. E. Coan,[1] V. Fadeyev,[1] I. Korolkov,[1] Y. Maravin,[1] I. Narsky,[1] R. Stroynowski,[1] J. Ye,[1] T. Wlodek,[1] M. Artuso,[2] E. Dambasuren,[2] S. Kopp,[2] G. C. Moneti,[2] R. Mountain,[2] S. Schuh,[2] T. Skwarnicki,[2] S. Stone,[2] A. Titov,[2] G. Viehhauser,[2] J.C. Wang,[2] J. Bartelt,[3] S. E. Csorna,[3] K. W. McLean,[3] S. Marka,[3] Z. Xu,[3] R. Godang,[4] K. Kinoshita,[4,*] I. C. Lai,[4] P. Pomianowski,[4] S. Schrenk,[4] G. Bonvicini,[5] D. Cinabro,[5] R. Greene,[5] L. P. Perera,[5] G. J. Zhou,[5] S. Chan,[6] G. Eigen,[6] E. Lipeles,[6] J. S. Miller,[6] M. Schmidtler,[6] A. Shapiro,[6] W. M. Sun,[6] J. Urheim,[6] A. J. Weinstein,[6] F. Würthwein,[6] D. E. Jaffe,[7] G. Masek,[7] H. P. Paar,[7] E. M. Potter,[7] S. Prell,[7] V. Sharma,[7] D. M. Asner,[8] J. Gronberg,[8] T. S. Hill,[8] C. M. Korte,[8] D. J. Lange,[8] R. J. Morrison,[8] H. N. Nelson,[8] T. K. Nelson,[8] D. Roberts,[8] H. Tajima,[8] B. H. Behrens,[9] W. T. Ford,[9] A. Gritsan,[9] H. Krieg,[9] J. Roy,[9] J. G. Smith,[9] J. P. Alexander,[10] R. Baker,[10] C. Bebek,[10] B. E. Berger,[10] K. Berkelman,[10] V. Boisvert,[10] D. G. Cassel,[10] D. S. Crowcroft,[10] M. Dickson,[10] S. von Dombrowski,[10] P. S. Drell,[10] K. M. Ecklund,[10] R. Ehrlich,[10] A. D. Foland,[10] P. Gaidarev,[10] L. Gibbons,[10] B. Gittelman,[10] S. W. Gray,[10] D. L. Hartill,[10] B. K. Heltsley,[10] P. I. Hopman,[10] J. Kandaswamy,[10] N. Katayama,[10] D. L. Kreinick,[10] T. Lee,[10] Y. Liu,[10] N. B. Mistry,[10] C. R. Ng,[10] E. Nordberg,[10] M. Ogg,[10,†] J. R. Patterson,[10] D. Peterson,[10] D. Riley,[10] A. Soffer,[10] B. Valant-Spaight,[10] A. Warburton,[10] C. Ward,[10] M. Athanas,[11] P. Avery,[11] C. D. Jones,[11] M. Lohner,[11] C. Prescott,[11] A. I. Rubiera,[11] J. Yelton,[11] J. Zheng,[11] G. Brandenburg,[12] R. A. Briere,[12] A. Ershov,[12] Y. S. Gao,[12] D. Y.-J. Kim,[12] R. Wilson,[12] H. Yamamoto,[12] T. E. Browder,[13] Y. Li,[13] J. L. Rodriguez,[13] S. K. Sahu,[13] T. Bergfeld,[14] B. I. Eisenstein,[14] J. Ernst,[14] G. E. Gladding,[14] G. D. Gollin,[14] R. M. Hans,[14] E. Johnson,[14] I. Karliner,[14] M. A. Marsh,[14] M. Palmer,[14] M. Selen,[14] J. J. Thaler,[14] K. W. Edwards,[15] A. Bellerive,[16] R. Janicek,[16] P. M. Patel,[16] A. J. Sadoff,[17] R. Ammar,[18] P. Baringer,[18] A. Bean,[18] D. Besson,[18] D. Coppage,[18] C. Darling,[18] R. Davis,[18] S. Kotov,[18] I. Kravchenko,[18] N. Kwak,[18] L. Zhou,[18] S. Anderson,[19] Y. Kubota,[19] S. J. Lee,[19] R. Mahapatra,[19] J. J. O'Neill,[19] R. Poling,[19] T. Riehle,[19] A. Smith,[19] M. S. Alam,[20] S. B. Athar,[20] Z. Ling,[20] A. H. Mahmood,[20] S. Timm,[20] F. Wappler,[20] A. Anastassov,[21] J. E. Duboscq,[21] K. K. Gan,[21] T. Hart,[21] K. Honscheid,[21] H. Kagan,[21] R. Kass,[21] J. Lee,[21] H. Schwarthoff,[21] A. Wolf,[21] M. M. Zoeller,[21] S. J. Richichi,[22] H. Severini,[22] P. Skubic,[22] A. Undrus,[22] M. Bishai,[23] S. Chen,[23] J. Fast,[23] J. W. Hinson,[23] N. Menon,[23] D. H. Miller,[23] E. I. Shibata,[23] I. P. J. Shipsey,[23] S. Glenn,[24] Y. Kwon,[24,‡] A.L. Lyon,[24] S. Roberts,[24] E. H. Thorndike,[24] C. P. Jessop,[25] K. Lingel,[25] H. Marsiske,[25] M. L. Perl,[25] V. Savinov,[25] D. Ugolini,[25] and X. Zhou[25]

[1]Southern Methodist University, Dallas, Texas 75275
[2]Syracuse University, Syracuse, New York 13244
[3]Vanderbilt University, Nashville, Tennessee 37235
[4]Virginia Polytechnic Institute and State University, Blacksburg, Virginia 24061

---

[*]Permanent address: University of Cincinnati, Cincinnati, OH 45221.

[†]Permanent address: University of Texas, Austin TX 78712.

[‡]Permanent address: Yonsei University, Seoul 120-749, Korea.

[5]Wayne State University, Detroit, Michigan 48202
[6]California Institute of Technology, Pasadena, California 91125
[7]University of California, San Diego, La Jolla, California 92093
[8]University of California, Santa Barbara, California 93106
[9]University of Colorado, Boulder, Colorado 80309-0390
[10]Cornell University, Ithaca, New York 14853
[11]University of Florida, Gainesville, Florida 32611
[12]Harvard University, Cambridge, Massachusetts 02138
[13]University of Hawaii at Manoa, Honolulu, Hawaii 96822
[14]University of Illinois, Urbana-Champaign, Illinois 61801
[15]Carleton University, Ottawa, Ontario, Canada K1S 5B6
and the Institute of Particle Physics, Canada
[16]McGill University, Montréal, Québec, Canada H3A 2T8
and the Institute of Particle Physics, Canada
[17]Ithaca College, Ithaca, New York 14850
[18]University of Kansas, Lawrence, Kansas 66045
[19]University of Minnesota, Minneapolis, Minnesota 55455
[20]State University of New York at Albany, Albany, New York 12222
[21]Ohio State University, Columbus, Ohio 43210
[22]University of Oklahoma, Norman, Oklahoma 73019
[23]Purdue University, West Lafayette, Indiana 47907
[24]University of Rochester, Rochester, New York 14627
[25]Stanford Linear Accelerator Center, Stanford University, Stanford, California 94309

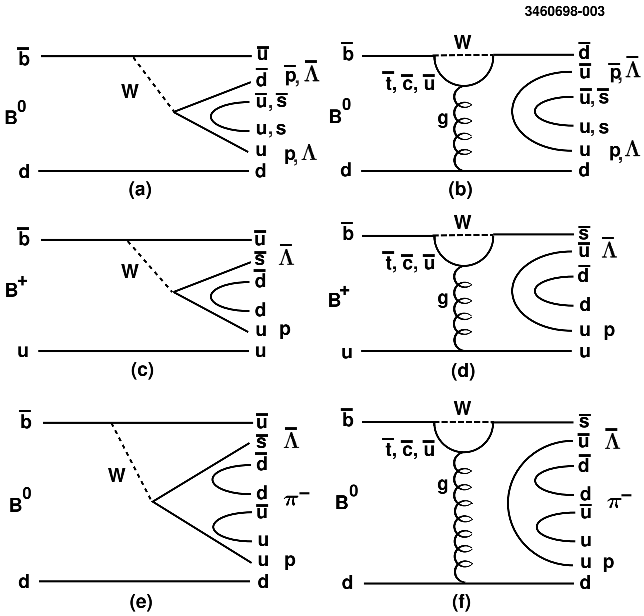

FIG. 1. Tree (a,c,e) and penguin (b,d,f) decay processes which are expected to dominate the baryonic decays under consideration.

Evidence for the $b \to s$ quark transition, allowed in the Standard Model by the penguin (internal W boson–quark loop) diagram, has been observed in both electromagnetic decays [1,2] and hadronic decays of B mesons to two mesons [3,4]. Charmless B meson decays can also arise through the $b \to u$ tree process as well as the Cabbibo suppressed $b \to d$ penguin process. These rare decay processes are of considerable theoretical and experimental interest due to their importance in probing the Cabibbo-Kobayashi-Maskawa (CKM) [5] picture of CP violation within the Standard Model.

This communication describes a search for charmless baryonic B decays to the final states $\Lambda\overline{\Lambda}$, $\overline{\Lambda}p$, $\overline{\Lambda}p\pi^-$, and $p\overline{p}$ (and their charge conjugate states). The dominant tree-level and one-loop penguin diagrams contributing to these decays are shown in Figure 1. The weak processes are similar to the meson decays $B \to \pi\pi$, $K\pi$, and KK. We expect $B^+ \to \overline{\Lambda}p$ and $B^0 \to \overline{\Lambda}p\pi^-$ to be dominated by the $b \to s$ penguin diagram, while $B^0 \to \Lambda\overline{\Lambda}$ and $B^0 \to p\overline{p}$ should be dominated by the $b \to u$ tree process. W-exchange, annihilation, penguin annihilation, and electroweak penguin processes can also contribute to these decay amplitudes [6]. However, these diagrams are expected to have small contributions as compared to those shown in Figure 1. Theoretical predictions for these modes, scaled for a common value of $|V_{ub}| = 0.0033$ [7], are given in Table I. Both pole model [8] and QCD sum rule calculations [9] have been performed. The pole model calculations yield higher predicted branching fractions for the rare baryonic modes. The search for the three-body final state $\overline{\Lambda}p\pi^-$ is motivated by the experimental observation that $\mathcal{B}(B^- \to \Lambda_c^+\overline{p}\pi^-)/\mathcal{B}(\overline{B^0} \to \Lambda_c^+\overline{p}) > 1.0$ (90% CL) [10]. We estimate the branching fraction for $\overline{\Lambda}p\pi^-$ from the measured branching fraction of $B^- \to \Lambda_c^+\overline{p}\pi^-$, scaling by the appropriate CKM and phase space factors. Penguin contributions could lead to significant enhancement over this rough estimate.

The data sets used in this analysis were collected with the CLEO II [11] detector at the

Cornell Electron Storage Ring (CESR). It consists of 5.41 fb^{-1} taken on the $\Upsilon(4S)$ resonance and 2.79 fb^{-1} taken below the $B\bar{B}$ production threshold. The on-resonance sample contains 3.3 million $B\bar{B}$ pairs taken before the installation of the silicon vertex detector, [12] (CLEO II data set) with the remainder of the 5.8 million $B\bar{B}$ pairs taken after the detector upgrade (CLEO II.V data set).

The momenta of charged particles are measured in a 67-layer tracking system operating inside a 1.5 T superconducting solenoid. The main drift chamber also provides a measurement of the specific ionization loss, dE/dx, which is used for particle identification. Photons are detected by the 7800-crystal CsI calorimeter. Muons are identified using proportional counters placed at various depths in the steel return yoke of the magnet.

Charged tracks are required to pass track quality requirements based on the average hit residual and the impact parameters in both the $r-\phi$ and $r-z$ planes. Pairs of tracks with vertices displaced by at least 5 mm from the primary interaction point are taken as Λ candidates. We require the $p\pi^-$ invariant mass to be within 10 MeV/c^2 of the Λ mass. Reconstructed Λ baryons have a mass resolution of 1.4 MeV/c^2. The impact parameter and Λ flight distance requirements nearly eliminate feed-across between the $\Lambda\overline{\Lambda}$ and $\overline{\Lambda}p\pi^-$ final states.

Charged particles are identified as protons or pions from specific ionization (dE/dx) measurements from the drift chamber. Electrons are rejected based on their dE/dx and the ratio of the track momentum to the associated shower energy in the CsI calorimeter. We reject muons by requiring that the tracks do not penetrate the steel absorber to a depth greater than five nuclear interaction lengths. For the $p\overline{p}$ final state, a requirement on the time-of-flight of the protons and antiprotons is applied that eliminates 40% of pion and 28% of kaon background while retaining 89% of the signal.

We calculate a beam-constrained B mass $M_{BC} = \sqrt{E_\mathrm{b}^2 - \mathbf{p}_B^2}$, where $\mathbf{p}_B$ is the B candidate momentum and E_b is the beam energy. The M_{BC} resolution is about 2.5 MeV/c^2 for all modes. We can capitalize on energy conservation if we define $\Delta E = \sum_i(E_i) - E_\mathrm{b}$, where E_i are the energies of the daughters that form the B meson candidate. The ΔE distribution is then centered about zero for reconstructed B mesons and has a mode-dependent Gaussian width that ranges from 17 MeV (for $\overline{\Lambda}p\pi^-$) to 25 MeV (for $p\overline{p}$). We accept events with M_{BC} within $5.2-5.3$ GeV/c^2 and $|\Delta E| < 200$ MeV. This region includes signal as well as a sideband used to fix the background normalization.

Backgrounds from $b \to c$ as well as other $b \to u$ and $b \to s$ decays are negligible for the two-body decay modes, since the signal daughter particles are relatively light and are produced with high momentum. This is in contrast to the dominant B meson decays which typically have a large number of final state particles with lower momenta. The decays $B^0 \to K^+\pi^-$ and $B^0 \to \pi^+\pi^-$ are displaced from zero by +287 and +330 MeV in ΔE, respectively, and do not pass the sideband ΔE requirements for the $p\overline{p}$ final state. Possible backgrounds from B decays to pseudoscalar-vector final states ($B \to PV$) such as $B \to \rho\pi$ and $B \to K^*\pi$ are found in simulation studies to contribute at most 4 ± 4 events to $p\overline{p}$. The simulations are normalized to 90% CL upper limits for $\mathcal{B}(B \to PV)$ [13]. For the three-body mode $\overline{\Lambda}p\pi^-$, we suppress backgrounds from B meson decays as well as continuum by requiring that the p, π^-, and Λ momentum be greater than 0.70, 0.75, and 1.0 GeV/c, respectively. The placement of these cuts was determined by a signal squared over background optimization.

TABLE I. Experimental results and theoretical predictions [8,9]. Branching fraction ($\mathcal{B}$) upper limits at 90% CL are given in 10^{-6} units with (without) systematic errors included. Quoted significance of the fit result is statistical only.

Mode	s	Sig.	$\mathcal{E}(\%)$	$\mathcal{B}$	Theory $\mathcal{B}$
$\Lambda\overline{\Lambda}$	$0.0^{+0.6}_{-0.0}$	0.0σ	14.8 ± 1.8	< 3.9 (3.4)	0.13
$p\overline{p}$	$12.1^{+6.0}_{-4.9}$	2.8σ	48.8 ± 2.7	< 7.0 (6.0)	0.6–4.8
$\overline{\Lambda}p$	$0.0^{+0.9}_{-0.0}$	0.0σ	29.3 ± 2.8	< 2.6 (2.3)	$\simeq 3$
$\overline{\Lambda}p\pi^-$	$3.0^{+3.8}_{-2.9}$	1.1σ	14.6 ± 1.7	< 13 (11)	$\simeq 0.5$

These requirements reduce the background from other B decays to less than 5% of the total background.

For this analysis, the main background arises from $e^+e^- \to q\bar{q}$ (where $q = u, d, s, c$). Such events typically exhibit a two-jet structure and produce high momentum back-to-back tracks. To reduce contamination from these events, we calculate the angle θ_{T} between the thrust axis of the candidate tracks and the thrust axis of the tracks and showers in the rest of the event. The distribution of $\cos\theta_{\mathrm{T}}$ is strongly peaked at ± 1 for $q\bar{q}$ events and is nearly flat for $B\bar{B}$ events. For the low background final state $\Lambda\overline{\Lambda}$, we require $|\cos\theta_{\mathrm{T}}| < 0.95$ and for the remaining modes we require $|\cos\theta_{\mathrm{T}}| < 0.9$. A cut of $|\cos\theta_{\mathrm{T}}| < 0.9$ eliminates 66% of continuum background while retaining 87% of the signal.

A detailed GEANT-based Monte Carlo (MC) simulation [14] was used to determine the overall detection efficiencies ($\mathcal{E}$) for each mode as shown in Table I. Efficiencies contain branching fractions for $\Lambda \to p\pi^-$ where applicable. For the efficiency calculation we assume that the decay $B^0 \to \overline{\Lambda}p\pi^-$ proceeds by phase space. [15] From independent Monte Carlo samples we estimate systematic errors on the efficiency determination; those errors are also given in Table I.

Additional discrimination between signal and $q\bar{q}$ background is provided by a Fisher discriminant technique, described in detail in Ref. [13]. The Fisher discriminant, $\mathcal{F} \equiv \sum_{i=1}^{11} \alpha_i y_i$, is a linear combination of 11 variables (y_i) where the coefficients (α_i) are chosen to maximize the separation between signal and background Monte Carlo samples. The input variables are $|\cos\theta_q|$ (the cosine of the angle between the candidate thrust axis and the beam axis), $|\cos\theta_B|$ (the cosine of the angle between the B meson momentum and the beam axis), and the energy and momentum contained within nine concentric 10° cones that surround the candidate thrust axis. The sum of energy and momenta from tracks and showers in the forward and backward cones are combined. The statistical separation between signal and continuum background afforded by the Fisher discriminant is 1.5 standard deviations (σ) after events with $|\cos\theta_{\mathrm{T}}| > 0.9$ have been rejected.

To determine the signal yield in each mode we perform an unbinned maximum likelihood (ML) fit using ΔE, M_{BC}, $\mathcal{F}$, Λ and $\overline{\Lambda}$ masses (where applicable), and dE/dx as input information for each candidate event. Separate fits are performed for each mode. The likelihood function is defined as

$$\mathcal{L} = e^{-(s+b)} \prod_{i=1}^{N} \left[s P_S(\vec{x_i}) + b P_B(\vec{x_i}) \right], \tag{1}$$

where s (b) are the signal (background) yields in the candidate sample (of N total events), P_S and P_B are the signal and background probability density functions (PDF), respectively, and $\vec{x_i}$ are the appropriate input variables discussed above. The signal and background yields are varied until the likelihood function is maximized. The probability density functions P_S and P_B are formed by the product of the best fit functional forms for signal and background distributions for each input variable. Signal MC is used to determine the shape of the signal events and off-resonance data is used to determine the background shapes. We use the sum of two Gaussians to parameterize the signal shapes for ΔE, M_{BC}, and Λ masses. Bifurcated Gaussians (with different low and high side widths) best describe the signal and background shapes for the Fisher discriminant and a straight line is used to parameterize the ΔE background shape and non-resonant Λ mass background. When determining the background M_{BC} distribution [16] the kinematic endpoint of the off-resonance data is matched to the on-resonance data by shifting the mass distribution by 5.290 GeV $- E_{\mathrm{b}}$.

Systematic errors on the fitted yields are determined by varying the PDFs used in the fit by their measurement errors. This variation is performed with a Monte Carlo technique in which the PDF parameters are varied by Gaussian distributed random numbers. The width of the Gaussian is equal to the measurement error of each parameter. For each variation the data sample is refit. The distribution of the fit yield and upper limit yield from these MC experiments is fit to a Gaussian whose width determines the ML fit systematic error. Important correlations between PDF parameters are accounted for in this technique.

For each of the four rare baryonic decay modes, Table I shows the signal yield (s) and statistical significance of the yield as determined from the likelihood function. Since we see no statistically significant signals in any of the modes, we calculate 90% confidence level upper limit yields (s^{UL}) by integrating the maximized likelihood function ($\mathcal{L}_{\max}$) as follows:

$$\frac{\int_0^{s^{UL}} \mathcal{L}_{\max}(N) dN}{\int_0^{\infty} \mathcal{L}_{\max}(N) dN} = 0.90. \tag{2}$$

The upper limit yield is then increased by its systematic error (from the PDF variation) and the detection efficiency reduced by its systematic error before we calculate the branching fraction upper limits shown in Table I. Table I also gives the upper limits for each mode before systematic errors have been included.

Figures 2 and 3 show the M_{BC} and ΔE projections, respectively, for each of the four modes. To reduce the background level in the plots we require $|\cos\theta_{\mathrm{T}}| < 0.8$ and apply a Fisher discriminant requirement, which eliminates roughly 80% of the background and retains about 60% of the signal. For the higher background modes ($\overline{\Lambda}p$, $\overline{\Lambda}p\pi^-$, and $p\overline{p}$) we require $|\Delta E| < 2.5\ \sigma_{\Delta E}$ for events to enter the M_{BC} plot and $|M_{BC} - 5.28| < 2.5\ \sigma_{M_{BC}}$ for events to enter the ΔE plot. Signal efficiency with these stricter requirements is about 50% of that quoted in Table I while background efficiency is only 1-3 %. Overlaid on these plots are the projections of the PDFs used in the fit, normalized according to the fit results multiplied by the efficiency of the additional constraints. Both signal and signal upper limit yields are illustrated in the figures.

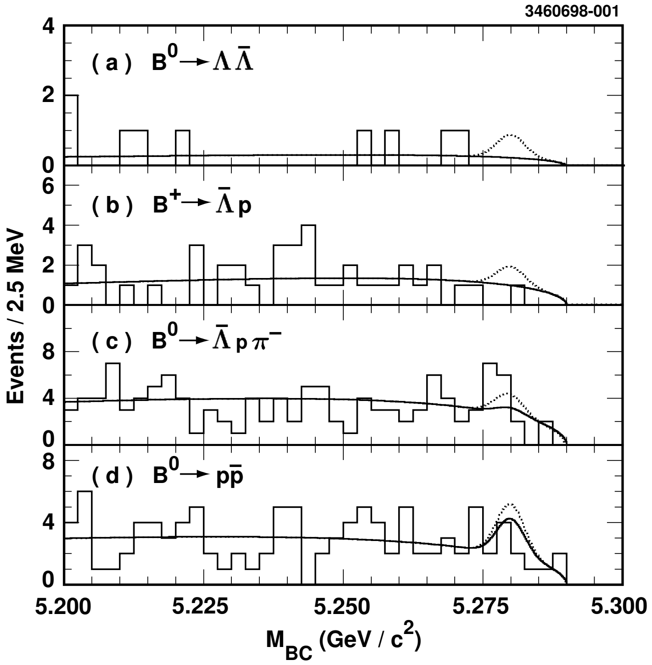

FIG. 2. M_{BC} projection plots for (a) $B^0 \to \Lambda\overline{\Lambda}$, (b) $B^+ \to \overline{\Lambda}p$, (c) $B^0 \to \overline{\Lambda}p\pi^-$, and (d) $B^0 \to p\overline{p}$. The scaled projection of the total likelihood fit (solid curve) and the fit reported upper limit (dotted curve) are overlaid.

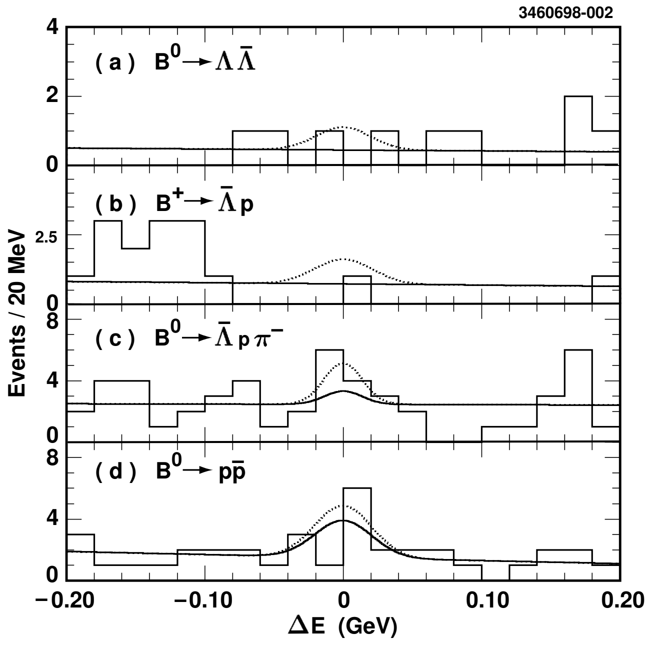

FIG. 3. ΔE projection plots for (a) $B^0 \to \Lambda\overline{\Lambda}$, (b) $B^+ \to \overline{\Lambda}p$, (c) $B^0 \to \overline{\Lambda}p\pi^-$, and (d) $B^0 \to p\overline{p}$. The scaled projection of the total likelihood fit (solid curve) and the fit reported upper limit (dotted curve) are overlaid.

We have searched for decays of B mesons to the baryonic final states $\Lambda\overline{\Lambda}$, $\overline{\Lambda}p$, $\overline{\Lambda}p\pi^-$, and $p\overline{p}$ (and charge conjugate states) in 5.8 million $B\overline{B}$ pairs collected with the CLEO detector. We see no statistically significant evidence for signals in any of these modes and set upper limits on their branching fractions. The upper limit for $B^+ \to \overline{\Lambda}p$ is slightly lower than the theoretical estimate given in Reference [9]. We see no evidence for $b \to s$ penguin transitions (recently observed in decays to meson final states) in B decays to baryonic final states.

We gratefully acknowledge the effort of the CESR staff in providing us with excellent luminosity and running conditions. J.R. Patterson and I.P.J. Shipsey thank the NYI program of the NSF, M. Selen thanks the PFF program of the NSF, M. Selen and H. Yamamoto thank the OJI program of DOE, J.R. Patterson, K. Honscheid, M. Selen and V. Sharma thank the A.P. Sloan Foundation, M. Selen and V. Sharma thank Research Corporation, S. von Dombrowski thanks the Swiss National Science Foundation, and H. Schwarthoff thanks the Alexander von Humboldt Stiftung for support. This work was supported by the National Science Foundation, the U.S. Department of Energy, and the Natural Sciences and Engineering Research Council of Canada.

REFERENCES

[1] M.S. Alam *et al.* (CLEO Collaboration), Phys. Rev. Lett **74**, 2885 (1995).
[2] R. Ammar *et al.* (CLEO Collaboration), Phys. Rev. Lett. **71**, 674 (1993).
[3] R. Godang *et al.* (CLEO Collaboration), Phys. Rev. Lett. **80**, 3456 (1998).
[4] B. Behrens *et al.* (CLEO Collaboration), Phys. Rev. Lett. **80**, 3710 (1998).
[5] M. Kobayashi and K. Maskawa, Prog. Theor. Phys. **49**, 652 (1973).
[6] Y. Kohara, Il Nuovo Cimento **104A**, 555 (1991).
[7] C. Caso *et al.* (Particle Data Group), "The 1998 Review of Particle Properties," *Eur. Phys. J.*, **C3**, 1 (1998).
[8] M. Jarfi *et al.*, Phys. Lett. B**237**, 513 (1990); M. Jarfi *et al.*, Phys Rev. D**43**, 1599 (1991); N. Deshpande, J. Trampetic, and A. Soni, Mod. Phys. Lett. **3A**, 749 (1988).
[9] V. Chernyak and I. Zhitnitsky, Nucl. Phys. B**345**, 137 (1990).
[10] X. Fu *et al.* (CLEO Collaboration), Phys. Rev. Lett. **79**, 3125 (1997).
[11] Y. Kubota *et al.* (CLEO Collaboration), Nucl. Instr. Methods Phys. Res. A**320**, 66 (1992).
[12] T. Hill, *Nucl. Instr. and Meth.*, **A418** (1998) 32
[13] D.M. Asner *et al.* (CLEO Collaboration), Phys. Rev. D **53**, 1039 (1996).
[14] R. Brun *et al.*, GEANT 3.15, CERN DD/EE/84-1.
[15] If the $\overline{\Lambda}p\pi^-$ final state were produced by the decay $B^0 \to \overline{\Lambda}\Delta^0$ with $\Delta^0 \to p\pi^-$, then the overall efficiency (including the $\Delta^0 \to p\pi^-$ branching fraction) decreases to $1.9 \pm 0.3\%$.
[16] We use the functional form $f(M_{BC}) \propto M_{BC}\sqrt{1-x^2}\exp[-\lambda(1-x^2)]$ where $x = M_{BC}/E_{\rm b}$ and λ is a fitted parameter. See H. Albrecht *et al.*, Phys. Lett. B **241**, 278 (1990); H. Albrecht *et al.*, Phys. Lett. B **254**, 288 (1991)